# **Inviscid and viscous flow past embedded planets**: implications for planet formation

Chris Ormel[a,b], Ji-Ming Shi[a]

[a]UC Berkeley, [b]Hubble Fellow

## Motivation, Goals, and Summary

**Context**
We have investigated the flow pattern that arises past (proto)planets embedded in a gaseous disk [6]. We consider a regime where the planet mass is large enough to gravitationally perturb the gas, but not too large to open gaps or accrete unlimited amounts of gas from the disk. Planets that are dominated by a rocky/icy core, like Neptune or the ubiquitously discovered super-Earths, fall in this mass regime.

**Statement of the problem and goals**
We consider a configuration in which the flow is steady in a frame that co-rotates with the planet, which is assumed to move in a circular orbit. Can we give a generic description of the steady flow pattern (density and velocity of the gas) as function of planet mass and disk properties? Can we distinguish between gas that belongs to the planet (the atmosphere) and the disk material? How does the headwind, caused by radial pressure gradient in the disk, affect the flow pattern?

**Strategy/Numerical details**
We concentrate on the region in the vicinity of the planet, i.e., on scales of the Bondi radius $R_b$: the radius where the thermal motions of the gas become similar to the escape velocity from the planet. Therefore, we do not use a softening parameter $r_s$ or else choose it to be very small ($r_s \ll R_b$). The outer domain size is typically limited to ~0.5 of the gas scaleheight so that contributions from Lindblad torques are ignored.

**Findings and Conclusions**
In (A) we consider the inviscid case and assume that the flow is barotropic, subsonic, 2D, but compressible. In that case a stream function ($\Psi$) formulation is feasible [3]. We solve for $\Psi$ numerically and have also derived analytical approximations that closely match our numerical ones. We find a strong dependence of the flow pattern on the headwind of the disk.

In (B) we consider viscous hydro-simulations and focus on the circumplanetary disk region — i.e., the atmosphere part of the flow pattern. We find that the circumplanetary disk is dominated by pressure (instead of rotation) and that its structure can be understood in terms of a viscous-stress model.

**Implications for planet formation**
In (C) we consider some implications of our findings for planet formation. In the standard (classical) model planets are thought to grow large by coagulation of ~km-size bodies — planetesimals [10]. Yet, this planet formation scenario may fail, especially in the outer disk regions, because planetesimals accretion is too slow, the bodies are too weak [2], or are readily excited by turbulence [1,5].

Therefore, a perhaps more viable alternative is when small particles (say of mm/cm in size) are the building blocks through which planets grow big. In (C) we show that accretion rates can indeed become very high but that it is not necessarily an efficient mechanism.

## A Inviscid Flow calculations

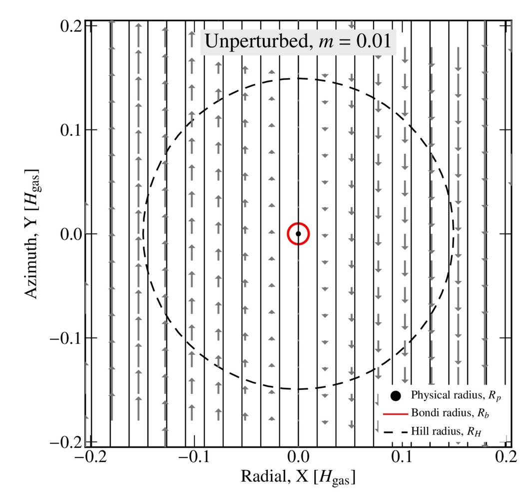


**Unperturbed state and units**
This figure plots the unperturbed flow pattern centered on the planet. The Keplerian-rotating gas moves in the azimuthal (y)-direction. The x-axis points away from the central star. The Keplerian shear causes the direction and magnitude of the flow to change.

The length unit is the scaleheight of the gas. The Hill radius is shown by the dashed circle; it gives the scale over which the solar gravity force is similar to the planet's gravity. The red circle represents the Bondi radius; it is the radius where the thermal motions of the gas equal the escape velocity from the planet. A strong increase in density can therefore be expeced beyond this radius. The dot at the very center denotes the physical radius of a planet.

We define a *dimensionless mass* $m = R_{bondi}/H_{gas}$. Below, we present results for m = 0.01, which corresponds approximately to an 0.1 Earth mass at 1 AU or to 10 $M_{Earth}$ at 10 AU.

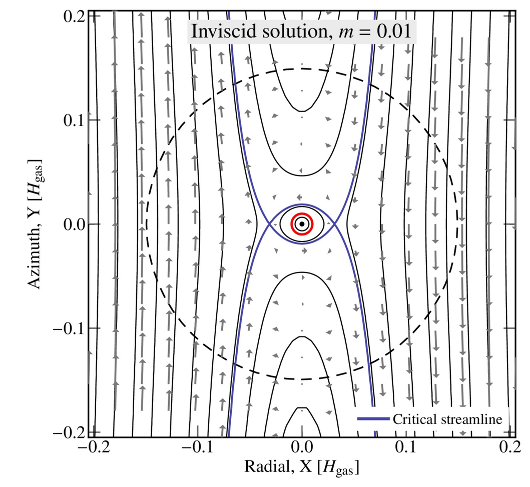


**Inviscous solution**
This figure shows the steady-state solution to the perturbed, inviscid flow. We identify 3 key regions:

(i) Only slightly perturbed flow at large |x|;
(ii) 'U-turn' flow at small |x|. This is the well-known horseshoe region;
(iii) Circulating flow at the very center on scales of the Bondi radius.

These three regions are separated by a critical streamline: the separatix (thick blue curve). Material that ends up in (iii) will never leave the planet. This is the atmosphere region. As one can see, the atmosphere covers several Bondi radii. The width of the horseshoe region (the distance between the critical streamlines) is consistent with the analysis of [8].

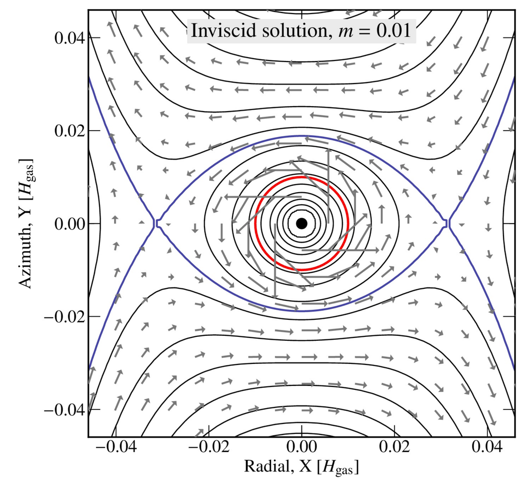


**Atmosphere**
We take a closer look at the flow near the atmosphere region. Within the atmosphere, the flow orbits the planet in the progade direction. This can be understood from the conservation of potential vorticity along streamlines:

$$PV = (\omega + 2)/\Sigma$$

where $\omega$ is the vorticity of flow and $\Sigma$ the surface density. In the unperturbed case, $\omega$ is negative (due to the Keplerian shear) but q is positive. Within the atmosphere region, however, $\Sigma$ becomes very large; subsequently the vorticity changes direction.

However, as the flow is circulating within the atmosphere (closed streamlines), there is ample time for viscous stresses to affect the flow pattern. This is investigated in (B).

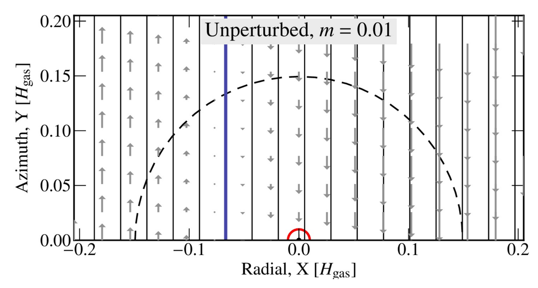


**Headwind/unperturbed**
We next consider the effects of a disk radial pressure gradient (due to variations in density and temperature), which causes the gas to move slower than Keplerian [12]. From its perspective, the Keplerian-moving planet faces a *headwind.*

The figure shows the unperturbed case for a headwind 10% of the sound speed. The dividing line between 'upwards' from 'downwards' flow has shifted inwards.

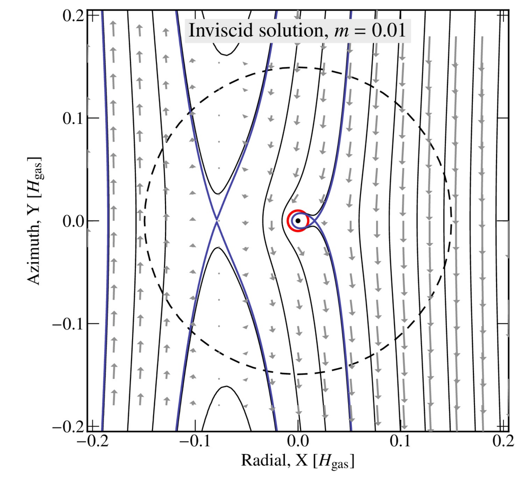


**Headwind solution**
The figure shows the solution of the flow including headwind. Comparing this soluiton to the non-zero headwind case above we find that the headwind flow breaks the symmetry. There are now several critical streamlines. One is associated with the horseshoe region, which is separated from the planet. Another one is associated with the planet's atmosphere.

(The inner-most streamline (near X = -0.2) is not associated with a critical point. It just happens that it has the same value of the stream function $\Psi$ as the streamline that marks the atmosphere.)

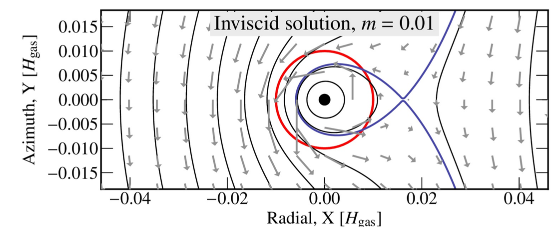


**Headwind/Atmosphere**
The atmosphere region is also much smaller than in the shear-only case. One sees that disk material passes w/i the planet's Bondi radius. This finding may have some implications for the thermodynamic structure of the atmosphere, as cold nebular disk material can penetrate it.

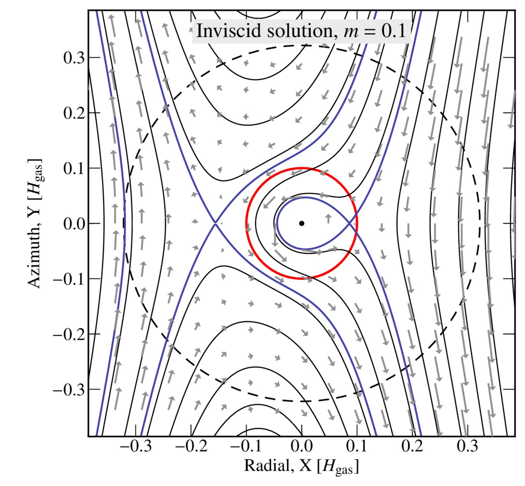


**A more massive planet**
All the above examples apply to a relatively small (proto)planet of m=0.01. A 10x more massive perturber, shown left, gives rise to a much wider horseshoe region, which lies closer to the planet. Note also that the Bondi radius (red circle) is a factor 10 larger (note the expanded scale of the box).

Nevertheless, the general features are the same as above. In the case with headwind the atmosphere stays relatively small, confined within the Bondi radius; it is still sandwiches between two streams of 'downward' moving nebular gas.

## B Viscous hydro-simulations

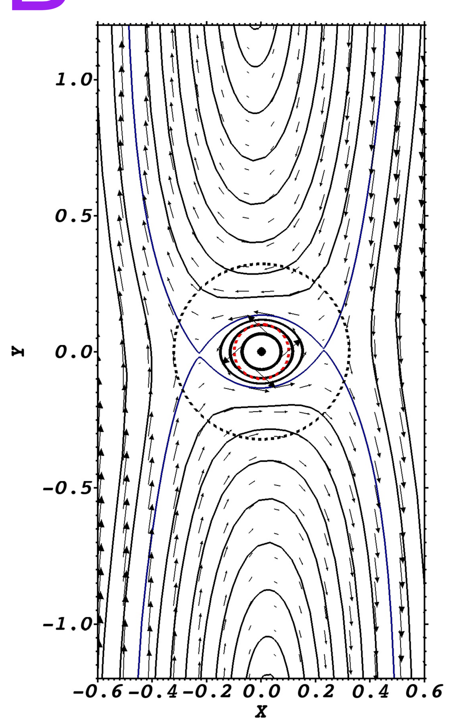


**Athena simulations**
We are conducting hydro simulations with *Athena* [11]. These simulations have a similar setup to those considered in (A), but do include a viscosity. In order to accurately resolve the flow near the planet we choose a smoothing parameter smaller than the Bondi radius, on the order of the grid spacing. We adopt a dimensionless mass parameter m = 0.1 (see (A)) and a kinematic viscosity $\nu = 10^{-3} c_s H_{gas}$.

The figure to the left shows the flow pattern in terms of streamlines and velocity arrows. These results are generally consistent with the inviscid calculations of (A).

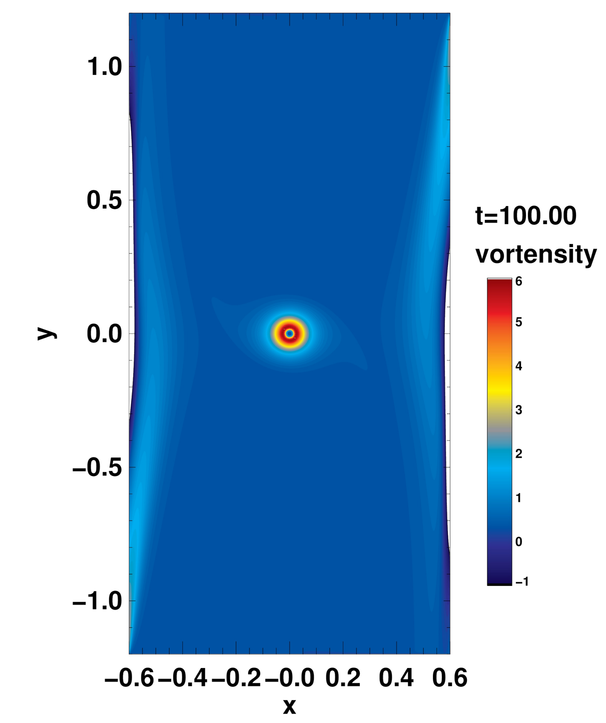


**Potential vorticity**
Here we show the potential vorticity (PV) of the flow. In the inviscid case the PV is expected to be 0.5Ω. This value is generally maintained within the co-orbital region. Deviations can be attributed to inaccurate boundary conditions and the onset of a spiral density wave.

Within the central atmosphere region the PV however becomes much larger than 0.5Ω. Within this region viscous stresses dominate the density and velocity structure, altering the PV.

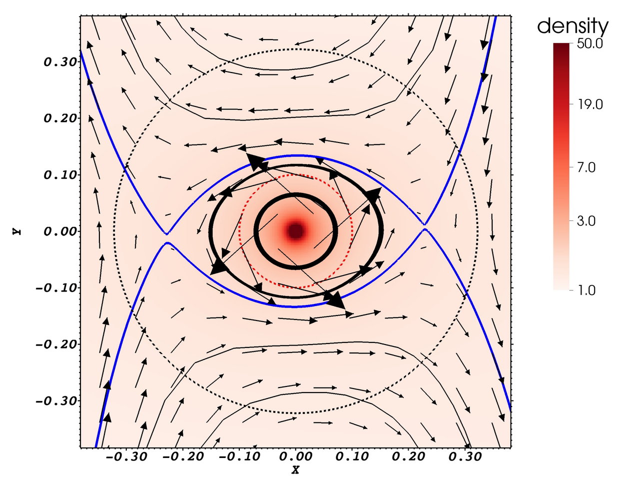


**Atmosphere region**
This figure shows a zoom in of the atmosphere region. The color denotes gas densities, which range from 1 to 50 on a logarithmic scale.

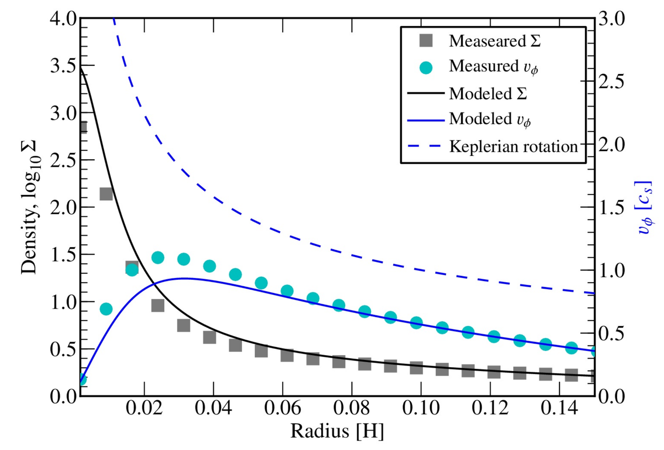


**Analysis**
This figure plots the azimuthally-averaged surface density (Σ) and velocity ($v_\varphi$) of the atmosphere region as function of radius (symbols). The azimuthal velocity falls below Keplerian rotation (dashed line).

We can understand the behavior of Σ and $v_\varphi$ by assuming that viscous stresses are consistent with steady state (solid curves). The small deviations are due to our assumption of axisymmetry and neglect of fiducial forces (coriolis force and tidal force) in this analysis.

## C Efficient accretion of small particles

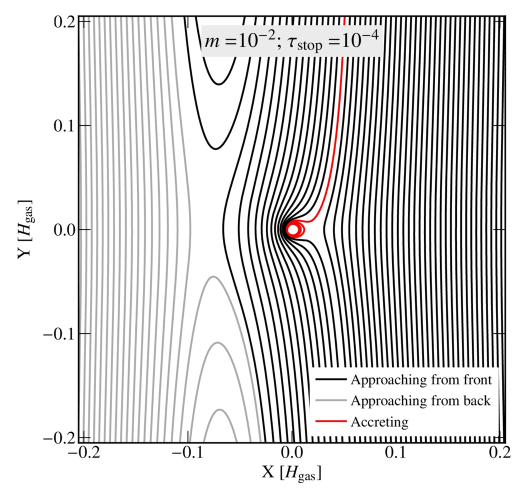


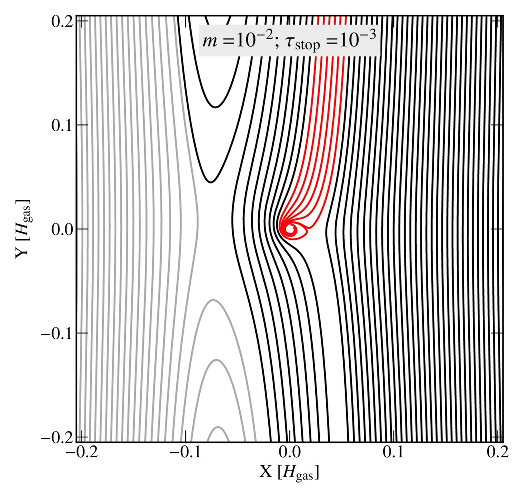


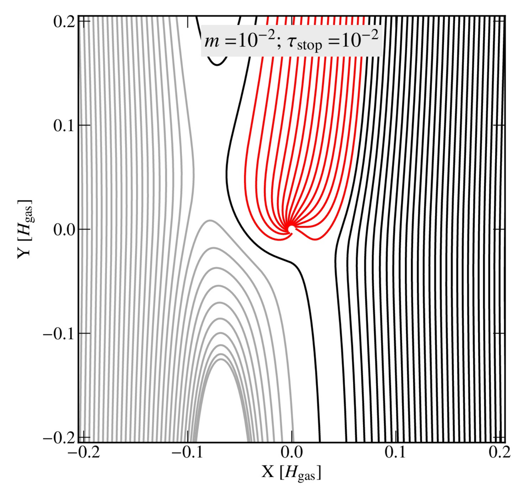


**Particle streams**
These figures show results of orbital integrations, in which a solid dust particle interacts with the planet. For small particles such interactions are strongly regulated by gas drag [4,7,9], for which we adopt the findings in (A) for an m = 0.01 planet and include a headwind.

The aerodynamic properties of small particles are identified by their stopping time $t_{stop}$, whose dimensionless equivalent is $\tau_{stop} = \Omega t_{stop}$. Here we consider stopping times in the $10^{-4}$—$10^{-2}$ range, which corresponds, roughly, to a size range of 0.1—10mm at 1 AU or 0.01—1mm at 10 AU.

The curves in the figures denote the trajectories of these particles — not those of the gas. Accreting trajectories are in red.

For small particles ($\tau_{stop} = 10^{-4}$) the trajectories are very similar to those of the gas — which is not unsurprising as their inertia is just very small. There is one stream (highlighted red), however, that enters the atmosphere and then starts to encircle the planet. These particles will eventually settle onto the planet.

For $\tau_{stop} = 10^{-3}$ and $\tau_{stop} = 10^{-2}$ particles the fraction that enters the atmosphere increases steeply. Also, particles start to deviate stronger from the gas flow.

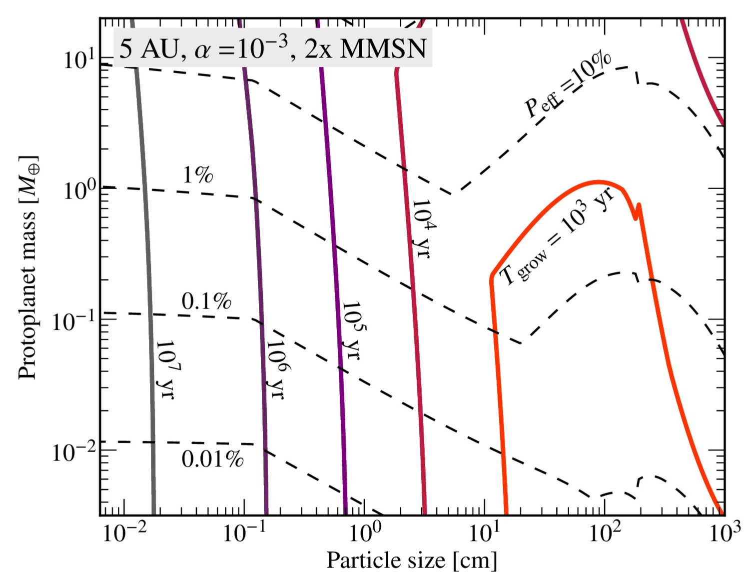


**Growth timescales and efficiency**
We consider a scenario where a protoplanet of mass $M_p$ (y-axis) sweeps up small particles (x-axis). The figure shows isocontours of the growth time-scale — the time required to double in mass (colored curves). It assumes that the surface density in solids is entirely composed of particles of a single size. The disk mass is considered to be 2x more massive than the minimum-solar mass and the protoplanet is located at 5 AU.

Growth timescales can be very short: less than 1000 years! Timescales increase for smaller particles though, because they are more thightly coupled to the (non-accreting) gas.

Two key factors limit the accretion rate. Firstly, vertical diffusion of particles, due to turbulence, decreases their spatial density in the (midplane) region. Secondly, due to the headwind, particles drift inwards [12] and there is only a limited time during which particles can get captured. This *accretion probability* (the likelihood of getting captured) is plotted by dashed lines.

Altogether, these findings show that the accretion rates and timescales are strong functions of planet mass and particle size, but also depend sensitively on the (local) properties of the gaseous disk (density, turbulence, headwind).

## References

[1] Gressel, O., Nelson, R. P., & Turner, N. J. (2012), MNRAS, 422... 1140
[2] Kobayashi H., Tanaka H., Krivov A. V. (2011), ApJ, 738... 35
[3] Korycansky D. G. and Papaloizou J. C. B. (1996), ApJS, 105... 181
[4] Lambrechts M. and Johansen A. (2012), A&A, 544... A32
[5] Ormel C. W. and Okuzumi S. (2013), ApJ in press
[6] Ormel C. W. (2013), MNRAS, 428... 3526
[7] Ormel C. W., Klahr H. H., (2010), A&A, 520... A43
[8] Paardekooper S.-J., Papaloizou J. C. B. (2009), MNRAS, 394... 2297
[9] Perets H. B., Murray-Clay R. A. (2011) ApJ, 733... 56
[10] Pollack, J. B., Hubickyj, O., Bodenheimer, P., et al. (1996), Icarus, 124... 62
[11] Stone J. M., Gardiner T. A.; Teuben P., Hawley J. F., Simon J. B., ApJS, 178... 137
[12] Weidenschilling S. J. (1977), MNRAS, 180... 57